Strain sensing using carbon fiber

Xiaojun Wang, Xuli Fu, and D. D. L. Chung
Composite Materials Research Laboratory, State University of New York at Buffalo, Buffalo, New York 14260-4400

(Received 15 September 1997; accepted 17 August 1998)

Carbon fiber provides strain sensing through change in electrical resistance upon strain. Due to piezoresistivity of various origins, a single carbon fiber in epoxy, an epoxy-matrix composite with short carbon fibers (5.5 vol%), a cement-matrix composite with short carbon fibers (0.2–0.5 vol%), and an epoxy-matrix composite with continuous carbon fibers (58 vol%) are strain sensors with fractional change in resistance per unit strain up to 625. A single bare carbon fiber is not piezoresistive, but just resistive.

I. INTRODUCTION

An important aspect of a smart structure is structural control, which typically involves the sensing of strain, displacement, or derivative quantities and the use of the signal from the sensor to activate certain actuators, which bring about the desired intelligent response of the structure. Thus, strain sensing is a key function in structural control. Numerous types of strain sensors are available, including optical fibers, piezoelectric sensors, electrostrictive sensors, magnetostrictive sensors, and piezoresistive sensors. The sensors are usually attached to or embedded in the structure.

Composite materials involving fiber reinforcements have become common structural materials. Among the various types of fibers, carbon fibers have become quite dominant due to their high strength, high modulus, low density, and temperature resistance. Carbon fibers are used to reinforce polymers, carbon, cement, and metals. If the carbon fibers in the composite provide strain sensing, then the conventional attached or embedded sensors are not necessary. This would mean reduced cost, greater durability, larger sensing volume, and absence of mechanical property degradation (due to embedded sensors). Therefore, this paper addresses strain sensing using carbon fibers.

Carbon fibers are electrically conductive. This behavior causes a change in electrical resistance in response to strain, thus enabling strain sensing. The nature of the electromechanical behavior depends on whether the fibers are continuous or discontinuous and depends on the matrix around the fibers. This paper provides a systematic study of the electromechanical behavior by considering (i) a single bare carbon fiber, (ii) a single carbon fiber in a matrix, (iii) a polymer-matrix composite containing randomly oriented short carbon fibers, (iv) a cement-matrix composite containing randomly oriented short carbon fibers, and (v) a polymer-matrix composite containing continuous unidirectional carbon fibers.

II. A SINGLE BARE CARBON FIBER

Previous electromechanical study of carbon fibers reported that, for low-modulus carbon fibers, the electrical resistance increases reversibly with tensile strain and decreases reversibly with compressive strain, mainly due to dimensional change rather than resistivity change.[1–5] The objective of this section is to investigate the electromechanical behavior of a single bare carbon fiber of the same type that is used in most of the following sections. In other words, this section provides baseline information that is needed for the following sections.

The carbon fiber used was 10E-Torayca T-300 (unsized, PAN-based) of diameter 7 μm, density 1.76 g/cm^3, tensile modulus 221 $\pm$ 4 GPa, tensile strength 3.1 $\pm$ 0.2 GPa, and ultimate elongation 1.4%. The electrical resistivity was (2.2 $\pm$ 0.5) $\times$ 10^{-3} Ω cm, as measured by using the four-probe method and silver paint electrical contacts on single fibers. Single fiber electromechanical testing was conducted by measuring the electrical resistance during static and cyclic tension. The dc resistance was measured by using the four-probe method, using silver paint for the electrical contacts. The outer two contacts (50 mm apart) were for passing a current; the inner two contacts (40 mm apart) were for voltage measurement (Fig. 1). A Keithley 2001 multimeter was used. Away from the four contacts, the single fiber was attached vertically with adhesive (60 mm apart) to a piece of paper with a rectangular hole cut in it (Fig. 1). Prior to vertical tension application, the paper was cut horizontally along the dashed lines shown in Fig. 1. The tension was under load control, as provided by a screw-type mechanical testing system (Sintech 2/D). The crosshead speed was 0.1 mm/min. The strain was obtained from the crosshead displacement.

Figure 2 shows typical plots of the fractional increase in resistance ($\Delta R/R_0$), stress, and strain simultaneously obtained during static tensile testing up to failure. $\Delta R/R_0$ increased monotonically with strain/stress,

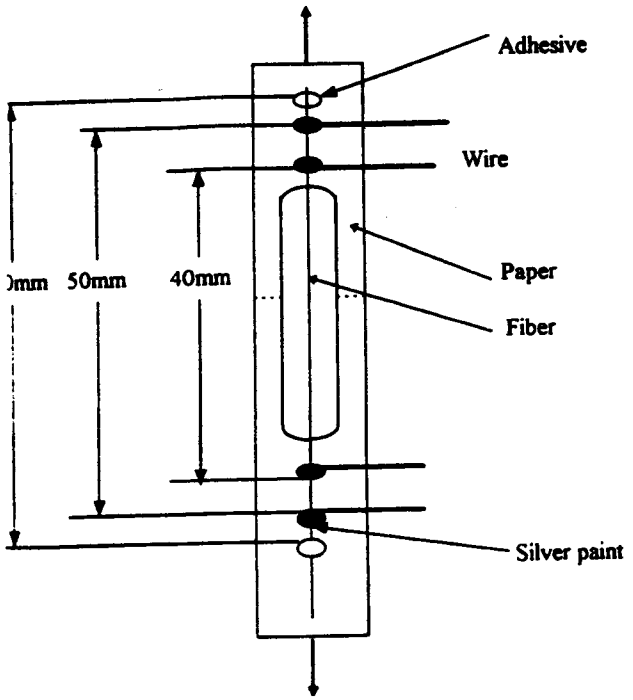

G. 1. Configuration for bare single fiber electromechanical testing. ıe single fiber is adhered to a sheet of paper using adhesive such that : points of adhesion are 40 mm apart. The four silver paint electrical ntacts are such that the outer contacts are 34 mm apart and the inner ntacts are 14 mm apart. The sheet of paper has a rectangular hole t in its middle. The inner contacts are within the hole.

ith a slight negative deviation from linearity. The gage ıctor (or strain sensitivity), given by the measured $\Delta R/R_0$ divided by the strain, was 1.8–1.9 throughout ıe whole range of strain. The $\Delta R/R_0$ calculated from ıe change in dimensions was less than but quite close) the measured $\Delta R/R_0$ at every strain value.

Figure 3 shows plots of $\Delta R/R_0$ versus time and ıain versus time, simultaneously obtained during the rst two cycles of tensile loading at stress amplitudes qual to 18.8, 58.1, and 83.0% of the fracture stress, re-pectively. The strain and $\Delta R/R_0$ were totally reversible t low values of the stress amplitude (up to 58.1% of ıe fracture stress), but their irreversible components ıcreased with stress amplitude at high values of the tress amplitude. At the highest stress amplitude of 3.0% of the fracture stress, the extent of irreversibil-ty of strain and $\Delta R/R_0$ increased slightly with cycle ıumber [Fig. 3(c)]. At the intermediate stress amplitude ıf 58.1% of the fracture stress, the strain was totally eversible but $\Delta R/R_0$ was not [Fig. 3(b)]. A nonzero ırreversible portion of $\Delta R/R_0$ was associated with a ıonzero fractional decrease in the elastic modulus from he first cycle to the second cycle. The greater the irre-ersible portion of $\Delta R/R_0$, the greater was the fractional lecrease in modulus. The gage factor, given by the eversible portion of $\Delta R/R_0$ divided by the reversible

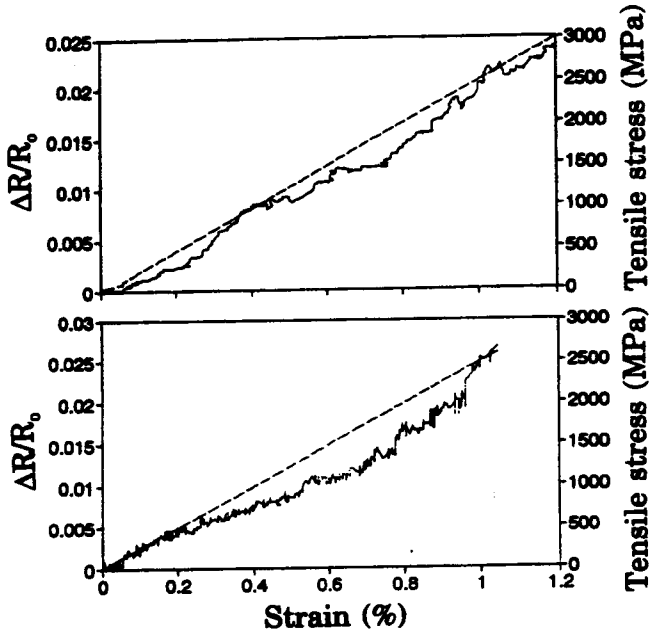

FIG. 2. $\Delta R/R_0$, stress, and strain simultaneously obtained during static tension up to failure of bare single fiber.

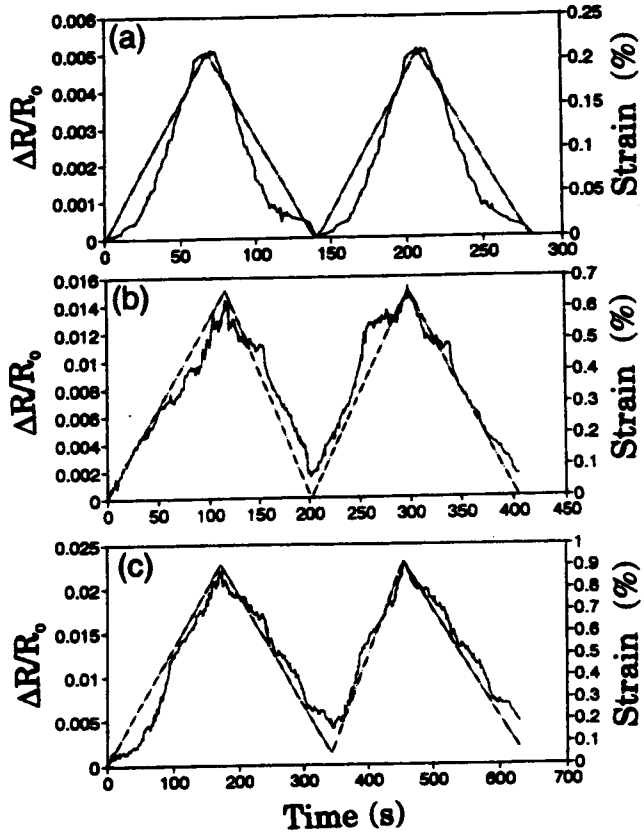

FIG. 3. Plots of $\Delta R/R_0$ versus time and of strain versus time during two cycles of cyclic tension of bare single fiber at a maximum stress of (a) 18.8% of the fracture stress, (b) 58.1% of the fracture stress, and (c) 83.0% of the fracture stress.

strain, was 1.9–2.3 at all stress amplitudes for both cycles 1 and 2. The $\Delta R/R_0$ calculated from the change in dimensions was less than the measured reversible $\Delta R/R_0$ at every stress amplitude.

Comparison of the calculated and measured reversible $\Delta R/R_0$ shows that dimensional change is the main cause of the observed reversible resistance change. The observed irreversible resistance change is attributed to damage, as supported by the accompanying decrease in the elastic modulus.

Even at a stress amplitude of 83.0% of the fracture stress, the irreversible portion of $\Delta R/R_0$ is much smaller than the reversible portion. Therefore, the use of the carbon fiber as a strain/stress sensor is possible. The irreversible portion, on the other hand, can be useful as an indicator of the amount of damage, so that the carbon fiber becomes a sensor of its own damage. This damage should be distinguished from fiber breakage, which would cause the irreversible $\Delta R/R_0$ to be ∞.

III. A SINGLE CARBON FIBER IN A MATRIX

In a composite, a carbon fiber is not bare but is embedded in a matrix. The objective of this section is to investigate the electromechanical behavior of a single carbon fiber embedded in a matrix. Two matrices are included, namely a polymer (i.e., epoxy) and a cement (i.e., portland cement, Type I).

A. In a polymer matrix

Resistive and piezoresistive behaviors are to be distinguished. Resistive behavior pertains to the reversible increase of the electrical resistance (not resistivity) of a fiber upon tensile strain, as described in Sec. II for a single bare carbon fiber. The piezoresistive behavior pertains to the reversible change in the electrical resistivity upon strain, as reported in this section for a single carbon fiber in epoxy.

It has been reported that a carbon fiber in epoxy increases its electrical resistivity during the curing of the epoxy due to the residual compressive stress resulting from the shrinkage during curing and thermal contraction during cooling of the epoxy.[5] Since the residual compressive stress in the fiber is expected to decrease upon subsequent tension of the fiber, this observation suggests that the electromechanical behavior of a carbon fiber in epoxy may be different from that of a bare carbon fiber. However, Ref. 5 reported the same electromechanical behavior for bare carbon fiber and carbon fiber in epoxy. As the residual compressive stress in a fiber increases with increasing curing temperature,[5] a higher curing temperature than Ref. 5 was used in this work. Consequently, the fiber resistivity (also resistance) increased by 10% after curing of epoxy in this work, whereas the fiber resistance increased by only 0.5% after room temperature curing in Ref. 5. Thus, upon subsequent tension of the fiber in cured epoxy, we observed decrease of the fiber resistance due to reduction of the residual compressive stress, whereas Ref. 5 observed increase of the fiber resistance (as in the case of the bare fiber). Our effect is a piezoresistive effect in which the resistivity of a carbon fiber in cured epoxy decreases reversibly upon tension of the fiber.

The carbon fiber used was 10E-Torayca T-300 (unsized, PAN-based). The epoxy used was EPON(R) resin 9405 together with curing agent 9470, both from Shell Chemical Co., in weight ratio 70 : 30. The recommended curing temperature is 150–180 °C for this epoxy.

The electrical resistance of a carbon fiber embedded in epoxy before and after the curing of the epoxy (at 180 °C, without pressure, for 2 h), as well as during subsequent tensile loading, was measured using the sample configuration of Fig. 4. A single fiber was embedded in epoxy for a length of 60 mm and an epoxy coating thickness of 5 mm, such that both ends of the fiber protruded and were bare in order to allow electrical contacts to be made on the fiber using silver paint. Four contacts (labeled A, B, C, and D in Fig. 4) were made. The outer two contacts (A and D) were for passing a current, whereas the inner two contacts (B and C, 80 mm apart) were for measuring the voltage. A Keithley 2001 multimeter was used for dc electrical measurements. The same electrical contact design was used in Sec. II for a single bare carbon fiber.

The electrical resistivity of carbon fiber increased by ~10% after curing and subsequent cooling. The fractional resistance increase was also ~10%.

It is known that the disparate thermal expansion properties of carbon fiber and epoxy leads to a residual thermal stress during the matrix (epoxy) solidification and subsequent cooling. Here we consider only the residual stress along the fiber direction (one dimension).

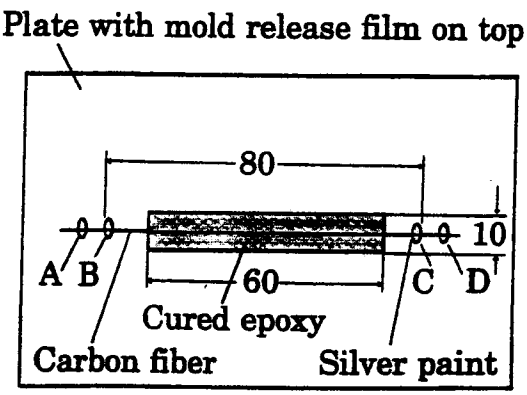

FIG. 4. Sketch of the resistance measurement setup for single carbon fiber embedded in epoxy. A, B, C, and D are four probes. A and D are for passing current; B and C are for voltage measurement. Dimensions are in mm.

Assuming that the strains of matrix and fiber are the same (if adhesion is perfect), and noting that there is no external force on the specimen, the residual thermal stress in the fiber is calculated to be 1438 MPa. In this case of single fiber in epoxy, the high residual stress is built up during curing and subsequent cooling. The observed resistance increase after curing and cooling is attributed to this residual stress.

Electromechanical testing of a single fiber in cured epoxy was conducted using the configuration of Fig. 4 during tension under load control, as provided by a screw-type mechanical testing system (Sintech 2/D). The crosshead speed was 0.1 mm/min. The strain was obtained from the crosshead displacement.

Figure 5 shows the fractional change in resistance ($\Delta R/R_0$) of fiber in cured epoxy upon static tension up to fiber fracture. Because of the small strains involved, $\Delta R/R_0$ was essentially equal to the fractional change in resistivity. The $\Delta R/R_0$ decreased by up to ~10% upon tension to a strain of ~0.5% (a stress of 1320 MPa) and then increased upon further tension. The magnitude of resistance decrease of carbon fiber in initial tension is close to the value of the prior resistance increase during curing and cooling of epoxy. The stress at which the resistance decrease was complete (1320 MPa) is close to the calculated value of 1438 MPa. Therefore, the initial decrease in $\Delta R/R_0$ in Fig. 5 is attributed to the reduction of the residual compressive stress in the fiber; the later increase is attributed to damage in the fiber. Section II on the electromechanical behavior of a bare carbon fiber has shown that damage causes the resistivity of the fiber to increase.

Figure 6 shows the $\Delta R/R_0$ of fiber in cured epoxy upon tensile loading to a strain of ~0.3% and upon subsequent unloading. The $\Delta R/R_0$ decreased upon loading and increased back to the initial value upon unloading, indicating the reversibility of the electromechanical effect.

The $\Delta R/R_0$ per unit strain for the electromechanical effect of Fig. 6 is −17. In contrast, $\Delta R/R_0$ per unit strain for the electromechanical effect associated with a bare carbon fiber and due to dimensional changes is 2. The large magnitude of $\Delta R/R_0$ per unit strain (called strain sensitivity or gage factor) for the new electromechanical effect of this section makes this effect technologically attractive.

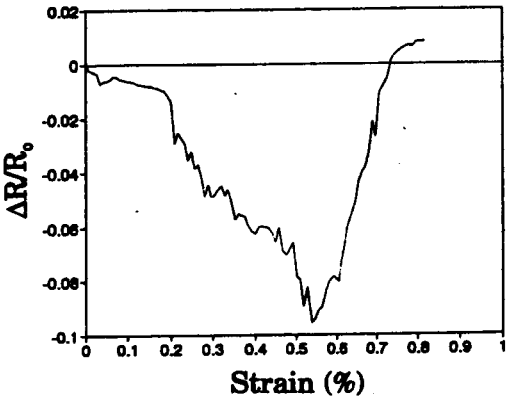

FIG. 5. The fractional electrical resistance change of single carbon fiber in epoxy under tension.

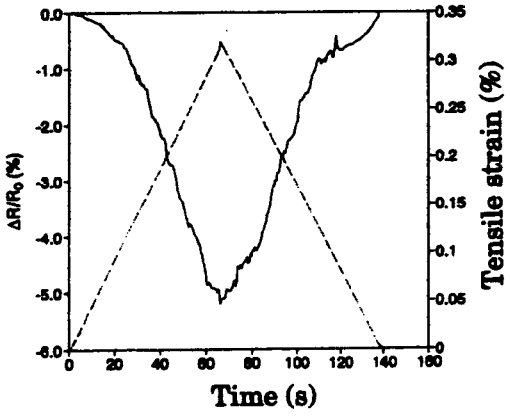

FIG. 6. Plots of $\Delta R/R_0$ versus time and strain versus time during tensile loading and unloading for single carbon fiber embedded in epoxy. Solid curve: $\Delta R/R_0$ versus time. Dashed curve: tensile strain versus time.

B. In a cement matrix

A similar investigation using cement paste instead of polymer as the matrix embedding a single carbon fiber was conducted. The carbon fiber used was isotropic pitch based, unsized, 10 μm in diameter, 690 MPa in tensile strength, 48 GPa in tensile modulus, 1.4% in elongation at break, and 3.0×10^{-3} Ω cm in electrical resistivity, as obtained as Carboflex from Ashland Petroleum Co. (Ashland, KY). This low grade carbon fiber was chosen because low cost is essential for the concrete industry. Cement paste made from portland cement (Type I) from Lafarge Corp. (Southfield, MI) was used for the cementitious material. The water/cement ratio was 0.35. No aggregate (fine or coarse) was used. The water-reducing agent used in the amount of 0.5% by weight of cement was TAMOL SN (Rohm and Haas, Co., Philadelphia, PA), which contained 93–96% sodium salt of a condensed naphthalenesulfonic acid. The experimental configuration is similar to Fig. 4. The

electrical resistivity of the fiber did not change during curing (at relative humidity 40%) of the cement paste. Thus, the electromechanical effect shown in Figs. 5 and 6 for the case of a polymer matrix does not exist for the case of a cement matrix. This negative result for a cement matrix is consistent with the fact that the bond between fiber and matrix is much weaker for cement than epoxy and the fact that the cement curing took place at room temperature (in contrast to the 180 °C curing for epoxy).

IV. A POLYMER-MATRIX COMPOSITE CONTAINING RANDOMLY ORIENTED SHORT CARBON FIBERS

A composite with an electrically conductive discontinuous filler and a less conductive (or nonconductive) and quite ductile matrix (e.g., a polymer) is piezoresistive because strain changes the proximity between the conducting filler units, thus affecting the electrical resistivity. Tension increases the distance between the filler units, thus increasing the resistivity; compression decreases this distance, thus decreasing the resistivity.[6-10]

This section describes the piezoresistivity in a polymer-matrix composite with randomly oriented short carbon fibers. The electromechanical results of this section serve as a baseline for comparing with those of a cement-matrix composite with the same type of short fibers (Sec. V). The carbon fibers were isotropic pitch based, unsized, 5 mm long, and 3×10^{-3} Ω cm in electrical resistivity, as obtained from Ashland Petroleum Co., Ashland, KY. The polymer was epoxy [Epon(R) 862 bisphenol F/epichlorohydrin epoxy resin and 3274 curing agent (mixture of polyoxyalkyleneamine and nonyl phenol, from Shell Chemical Co.)]. The fiber volume fraction was 5.5 vol%. The composites were fabricated by mixing the fibers with the epoxy resin, putting the mixture in a rough vacuum to remove bubbles, and then curing at room temperature for 24 h.

Figure 7 shows the stress, strain, and fractional resistance increase ($\Delta R/R_0$) obtained simultaneously during cyclic tension to a maximum stress equal to 72% of the breaking stress. The strain is totally reversible. Because of the small strains involved, $\Delta R/R_0$ is essentially equal to the fractional increase in resistivity. The value of $\Delta R/R_0$ increases upon first tensile loading and then decreases upon unloading to a level above the initial zero value. Reloading causes $\Delta R/R_0$ to increase again, and subsequent unloading behaves in a manner similar to the first unloading. That $\Delta R/R_0$ does not return to the original value after the first cycle indicates the occurrence of irreversible damage during the first loading, even though the strain is totally reversible. Figure 7 shows that there are two portions to $\Delta R/R_0$—one portion is irreversible while the other portion is reversible. The irreversible portion increases with strain amplitude up to the highest strain amplitude used, whereas the reversible portion increases with strain amplitude up to a strain amplitude of 62% of the fracture strain. The irreversible portion exceeds the reversible portion at the lowest stress amplitude (27%), but is less than the reversible portion for all other stress amplitudes (44, 61, and 72%). Consistent with the cyclic tension results of Fig. 7 is the static tension result (up to fracture) of Fig. 8. The $\Delta R/R_0$ increases monotonically with strain up to fracture. At low strains, $\Delta R/R_0$ is mainly due to piezoresistivity; at high strains, $\Delta R/R_0$ is mainly due to fiber breakage.

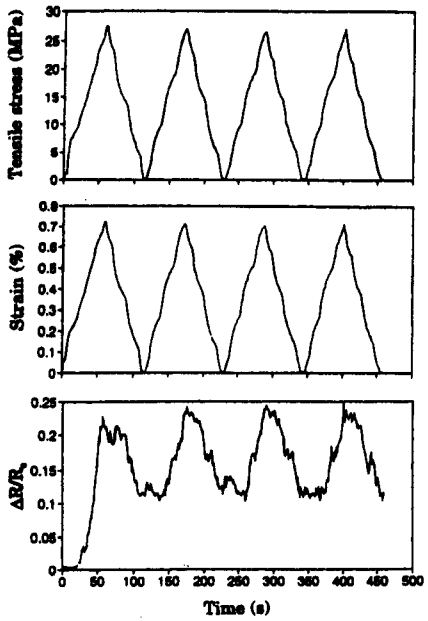

FIG. 7. Plots versus time of $\Delta R/R_0$ tensile strain, and tensile stress obtained during cyclic tensile testing at a stress amplitude of 75% for an epoxy-matrix composite with short carbon fibers.

Figure 9 shows the stress, strain, and $\Delta R/R_0$ obtained simultaneously during cyclic compression to a maximum stress equal to 27% of the breaking stress. The strain is totally reversible. Because of the small strains involved, $\Delta R/R_0$ is essentially equal to the fractional increase in resistivity. The value of $\Delta R/R_0$ decreases upon first compressive loading and then increases upon unloading to a level above the initial zero value. Reloading causes $\Delta R/R_0$ to decrease to the same low level as that during first loading and subsequent unloading causes $\Delta R/R_0$ to increase to the same high level as that after first unloading. Subsequent cycles are all similar in behavior. That $\Delta R/R_0$ does not return to the original zero value after the first cycle indicates the occurrence of irreversible damage during the first loading, even though the strain is totally reversible. Figure 9 shows that there are two portions of $\Delta R/R_0$—one portion is irreversible while the other portion is reversible. The magnitudes of both portions increase with strain amplitude up to the highest strain amplitude used. The irreversible portion is less than the magnitude of the reversible portion for all stress amplitudes. Consistent with the cyclic compression results of Fig. 9 is the static compression result (up to fracture) of Fig. 10. The $\Delta R/R_0$ decreases with strain up to 2.3% due to piezoresistivity and then increases with strain (probably due to fiber breakage) when the strain exceeds 2.3%.

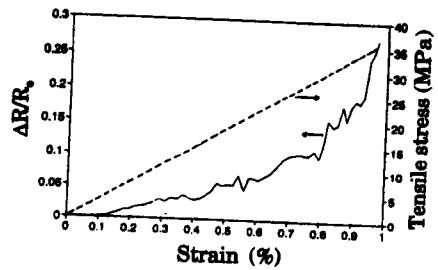

FIG. 8. Plots versus strain of tensile stress and $\Delta R/R_0$ during static tensile testing up to fracture for an epoxy-matrix composite with short carbon fibers.

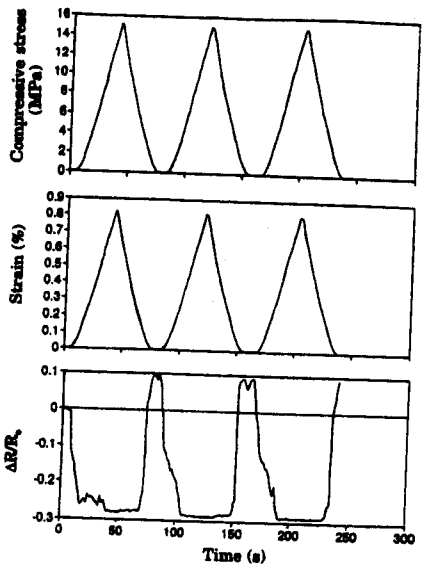

FIG. 9. Plots versus time of $\Delta R/R_0$, compressive strain, and compressive stress obtained during cyclic compressive testing at a stress amplitude of 27% for an epoxy-matrix composite with short carbon fibers.

The irreversible portions in Figs. 7 and 9 are attributed to damage, probably related to a fiber-matrix contact resistivity increase (interface weakening) rather than fiber breakage, since the stress-strain relationship does not change during cycling in Figs. 7 and 9. The reversible portions are attributed to piezoresistivity.

The gage factor is defined as the reversible portion of $\Delta R/R_0$ per unit strain. It is also known as the strain sensitivity. It is lower under tension than compression. Under compression, it (29–31) is essentially independent of the stress amplitude (ratio of the maximum stress to the fracture stress). Under tension, it (6–19) increases with stress amplitude up to 61%.

V. A CEMENT-MATRIX COMPOSITE CONTAINING RANDOMLY ORIENTED SHORT CARBON FIBERS

A cement matrix is more brittle than a polymer matrix, so the piezoresistivity originating from the change in proximity between the adjacent short fibers upon strain occurs for a polymer-matrix composite (Sec. IV), but not for a cement-matrix composite. Another origin of piezoresistivity applies to the cement-matrix composite with randomly oriented short carbon fibers that are of the same type as in Sec. IV for a polymer matrix. This other origin relates to the reversible and slight (<1 μm) fiber pullout (crack opening while fiber bridges the crack) and the consequent reversible increase in the electrical resistivity. This origin results in a gage factor as high as

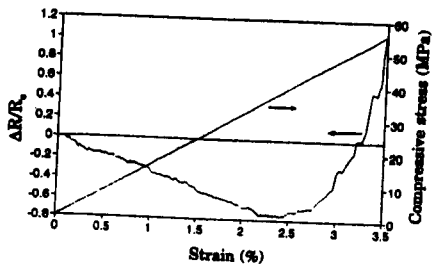

FIG. 10. Plots versus strain of compressive stress and $\Delta R/R_0$ during static compressive testing up to fracture for an epoxy-matrix composite with short carbon fibers.

500 under compression or tension, in contrast to values up to 31 for the polymer-matrix counterpart (Sec. IV). The evidence in support of this origin for the cement-matrix composite is summarized below.

(1) The sensing ability was present when the fibers were conducting (i.e., carbon or steel) and absent when the fibers were nonconducting (i.e., polyethylene).[11]

(2) The sensing ability was absent when fibers were absent.[11–14]

(3) The sensing ability occurred even at low carbon fiber volume fractions, which were associated with little effect of the fiber addition on the concrete's volume electrical resistivity.[11,15,16]

(4) There was no maximum volume electrical resistivity required in order for the sensing ability to be present.[11]

(5) The sensing ability was present when the carbon fiber volume fraction was as low as 0.2% (below the percolation threshold).[11,14]

(6) Fracture surface examination showed that the fibers were separate from one another.[11]

(7) The fractional increase in electrical resistance ($\Delta R/R_0$) upon straining essentially did not increase with increasing carbon fiber volume fraction, even though the increase in fiber volume fraction caused large decrease (by orders of magnitude) in the volume electrical resistivity.[11]

(8) The electrical resistance increased upon tension (fiber pullout) and decreased upon compression (fiber push-in) at any curing age, except for the first compressive strain cycle at less than 14 days of curing in which the resistance increased (Fig. 11). The resistance change during the first strain cycle was consistent with the need to weaken the fiber-matrix interface prior to fiber pullout in case the interface was strong to start with.[11,17,18]

(9) The presence of carbon fibers caused the crack height to decrease by orders of magnitude, as observed after deformation to 70% of the compressive strength.[11]

(10) The presence of carbon fibers caused the flexural toughness and tensile ductility of the composite to greatly increase.[16,19]

(11) The stress required for fiber pullout in the short fiber composite was consistent with the shear bond strength between carbon fiber and cement paste, as obtained by single fiber pullout testing.[20]

(12) The contact electrical resistivity between carbon fiber and cement paste increased during debonding.[20]

(13) The residual stress in a single carbon fiber embedded in cement paste is negligible (Sec. III).

Carbon fibers (same type and length as in Sec. IV) in the amount of 0.5% by weight of cement (corresponding to 0.51 vol% of composite) were used. Cement paste made from portland cement (Type I) from Lafarge Corp. (Southfield, MI) was used for the cementitious material. The water/cement ratio was 0.35. No aggregate was used. The water-reducing agent used in the amount of 3% by weight of cement was TAMOL SN (Rohm and Haas Co., Philadelphia, PA), which contained 93–96% sodium salt of a condensed naphthalenesulfonic acid. Methylcellulose and silica fume were added to help disperse the fibers. Silica fume (Elkem Materials Inc., Pittsburgh, PA, #965) was used in the amount of 15% by weight of cement. Methylcellulose (Methocel A15–LV, Dow Chemical Corporation, Midland, MI) in the amount of 0.4% by weight of cement was used together with a defoamer (Colloids 1010, Colloids, Inc., Marietta, GA) in the amount of 0.13 vol%.

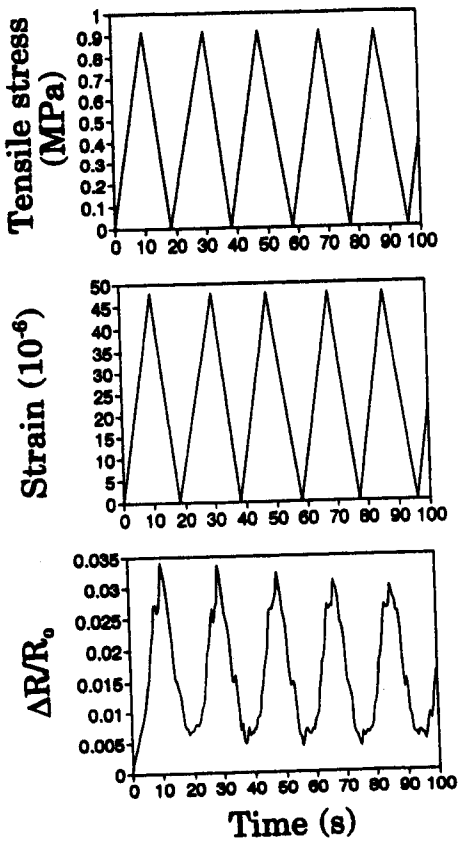

FIG. 11. $\Delta R/R_0$, strain, and stress during first cyclic tensile loading of cement paste at 28 days of curing.

Methylcellulose was dissolved in water and then fibers and defoamer were added and stirred by hand for about 2 min. Then this mixture, cement, water, water-reducing agent, silica fume, and sand (sand/cement ratio = 1.0; particle size analysis shown in Fig. 1 of Ref. 12; only for mortar, not for cement paste) were mixed in a Hobart mixer for 5 min. The mixer had a flat beater. After pouring the mix into oiled molds, a vibrator was used to decrease the amount of air bubbles. The specimens were demolded after 1 day and then allowed to cure at room temperature in air at a relative humidity of 40% for 28 days.

Simultaneous to mechanical testing, dc electrical resistance measurements were made (ac measurements showed that resistance and reactance varied with strain in qualitatively similar fashions). For compressive testing according to ASTM C109-80, specimens were prepared by using a 2 × 2 × 2 in. (5.1 × 5.1 × 5.1 cm) mold. Dog-bone-shaped specimens were used for tensile testing, as prepared by using molds of the same shape and size. The strain was measured by a strain gage under tension and by the crosshead displacement under compression, while the fractional change in electrical resistance along the stress axis was measured using the four-probe method. The electrical contacts were made by silver paint. Although the spacing between the contacts changed upon deformation, the change was so small that the measured resistance remained essentially proportional to the resistivity.

Figure 11 gives the fractional dc resistance increase ($\Delta R/R_0$) during first tensile loading of cement paste with 0.51 vol% carbon fibers at a stress amplitude of 0.9 MPa, or a strain amplitude of 4.8×10^{-5}, which was within the elastic regime, at 28 days of curing. (The tensile strength was 1.97 MPa.) The resistance was in the stress direction. Both stress and strain returned to zero at the end of each cycle. The $\Delta R/R_0$ increased during tensile loading in each cycle and decreased during unloading in each cycle, with a gage factor of 625. This is due to fiber pullout during loading and fiber push-in during unloading. At the end of the first cycle, $\Delta R/R_0$ was positive rather than zero. This resistance increase is attributed to damage of the fiber-cement interface due to the fiber pullout and push-in. As cycling progressed, both the maximum $\Delta R/R_0$ and minimum $\Delta R/R_0$ in a cycle decreased. This is attributed to damage of the cement matrix separating adjacent fibers at their junction; this damage increased the chance for adjacent fibers to touch one another, thereby decreasing the resistivity.

Figure 12 gives $\Delta R/R_0$ during first cyclic compressive loading of mortar with 0.24 vol% carbon fibers at a stress amplitude of 16 MPa, or a strain amplitude of 8×10^{-4}, which was within the elastic regime, at 28 days of curing. (The compressive strength was 45 MPa.) The resistance was in the stress direction. Both stress and strain returned to zero at the end of each cycle. The $\Delta R/R_0$ decreased during compressive loading in each cycle and increased during unloading in each cycle, with a gage factor of 500. This is due to fiber push-in during loading and fiber pullout during unloading. At the end of the first cycle, $\Delta R/R_0$ was positive rather than zero. This resistance increase is attributed to damage of the fiber-cement interface due to the fiber push-in and pullout. As cycling progressed, both the maximum $\Delta R/R_0$ and minimum $\Delta R/R_0$ in a cycle decreased. This is attributed to damage of the cement matrix separating adjacent fibers at their junction, as explained above. This decrease from cycle to cycle persisted for the first ~150 cycles

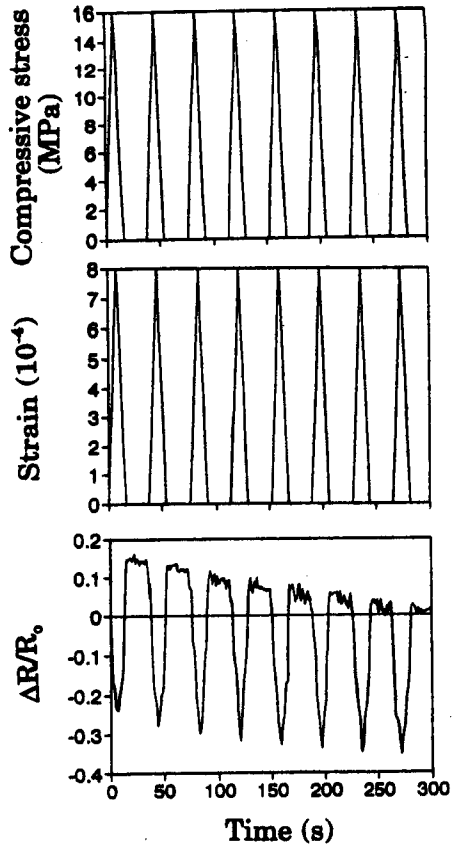

FIG. 12. $\Delta R/R_0$, strain, and stress during first cyclic compressive loading of mortar at 28 days of curing.

after which the maximum and minimum $\Delta R/R_0$ did not change with cycling.

The gradual decrease as cycling progressed of both maximum and minimum $\Delta R/R_0$ in a cycle occurred in both tension and compression. This effect is undesirable, as it degrades the repeatability of the sensing ability. However, it can be removed by using ozone treated carbon fibers.[21]

VI. A POLYMER-MATRIX COMPOSITE CONTAINING CONTINUOUS UNIDIRECTIONAL CARBON FIBERS

Section III describes the piezoresistivity of a single carbon fiber embedded in a polymer matrix. This section extends the work to a polymer-matrix composite[22] containing a large number of continuous unidirectional carbon fibers that are of the same type as in Sec. III for a single fiber in a polymer.

Composite samples were constructed from individual layers cut from a 12 in. (30.5 cm) wide unidirectional carbon fiber prepreg tape manufactured by ICI Fiberite (Tempe, AZ). The product used was Hy-E 1076E, which consisted of a 976 epoxy matrix and 10E carbon fibers. The composite laminates were laid up in a 4 × 7 in. (10.2 × 17.8 cm) platten compression mold with laminate configuration $[0]_8$ and $[0]_{24}$ for tensile and compressive specimens, respectively. The individual 4 × 7 in. fiber layers (8 per laminate for tensile specimens and 24 per laminate for compressive specimens) were cut from the prepreg tape. The layers were stacked in the mold with a mold release film on the top and bottom of the layup. No liquid mold release was used. The laminates were cured using a cycle based on the ICI Fiberite C-5 cure cycle. Heating occurred under pressure (89 psi or 0.56 MPa) at a rate of 1–5 °F/min. The curing occurred at 355 ± 10 °F (179 ± 6 °C) and 89 psi (0.61 MPa) for 120 ± 10 min. Subsequent cooling was at a maximum rate of 5 °F/min. Afterward, the laminates were cut to pieces of size 160 × 14 mm (thickness = 1.1 mm) for tensile testing and 60 × 6 mm (thickness = 3.3 mm) for compressive testing. For the $[0]_8$ laminate, the fiber volume fraction was 58%, the density was 1.52 ± 0.01 g/cm^3, the tensile strength in the fiber direction was 1268 ± 89 MPa, the tensile ductility was (1.08 ± 0.08)%, the Poisson ratio was 0.30, and the resistivity was 4.1×10^{-3} Ω cm in the fiber direction and 2.04 Ω cm in the through-thickness direction. With 6000 fibers per bundle and 7 μm diameter for a fiber, there were 38 fiber bundles in a tensile specimen. For tensile testing, glass fiber reinforced epoxy end tabs were applied to both ends on both sides of each cured piece, such that each tab was 30 mm long and the inner edges of the end tabs on the same side were 100 mm apart and the outer edges were 160 mm apart.

The volume electrical resistance R was measured using the four-probe method while cyclic tension or compression was applied in the longitudinal direction (parallel to fibers). Silver paint was used for all electrical contacts. The four probes consisted of two outer current probes and two inner voltage probes. The resistance R refers to the sample resistance between the inner probes. The longitudinal and through-thickness R were measured in different samples. For the longitudinal R measurement, the four electrical contacts were around the whole perimeter of the sample in four parallel planes that were perpendicular to the stress axis, such that the inner probes were 60 mm apart and the outer probes were 78 mm apart for the tensile specimens. For the through-thickness R measurement, the current contacts were centered on the largest opposite faces and in the form of open rectangles of length 80 mm in the longitudinal direction, while each of the two voltage contacts was in the form of a solid rectangle (of length 20 mm in the longitudinal direction) surrounded by a current contact (open rectangle). Thus, each face had a current contact surrounding a voltage contact. A resistive strain gage (Micromeasurements Group, #991117) was attached to the center of one of the largest opposite faces, for both longitudinal and transverse R measurement samples. In the case of the through-thickness R measurement sample, the strain gage was at the center of the inner rectangle (voltage contact). A Keithley 2001 multimeter was used. A hydraulic mechanical testing system (MTS 810) was used in both tensile and compressive testing with a displacement rate of 1.0 mm/min.

Figure 13 shows the longitudinal stress, strain, and fractional longitudinal resistance increase ($\Delta R/R_0$) obtained simultaneously during cyclic tension of the $[0]_8$ laminate to a stress amplitude equal to 14% of the breaking stress. The strain returned to zero at the end of each cycle. Because of the small strains involved, $\Delta R/R_0$ is essentially equal to the fractional increase in resistivity. The longitudinal $\Delta R/R_0$ decreased upon loading and increased upon unloading in every cycle, such that R irreversibly decreased slightly after the first cycle (i.e., $\Delta R/R_0$ did not return to 0 at the end of the first cycle). At higher stress amplitudes, the effect was similar, except that both the reversible and irreversible parts of $\Delta R/R_0$ were larger.

Figure 14(a) shows the longitudinal stress, strain, and $\Delta R/R_0$ obtained simultaneously during static longitudinal tensile loading up to fracture. The longitudinal $\Delta R/R_0$ first decreased until a strain of 0.6% and then increased in steps as the strain increased, due to fiber breakage. The decrease in $\Delta R/R_0$ in the low strain regime is consistent with the trend in Fig. 13. Figure 14(b) is a plot of the fraction of fibers broken versus strain, as obtained from Fig. 14(a) by noting that a broken fiber is incapable of electrical conduction.

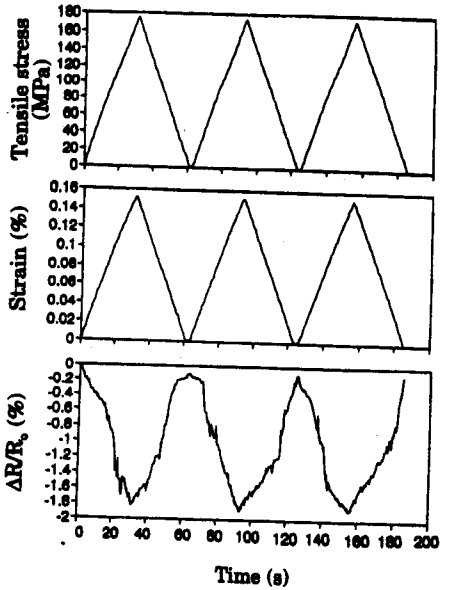

FIG. 13. Longitudinal stress and strain and fractional resistance increase ($\Delta R/R_0$) obtained simultaneously during cyclic tension at a stress amplitude equal to 14% of the breaking stress for continuous fiber epoxy-matrix composite.

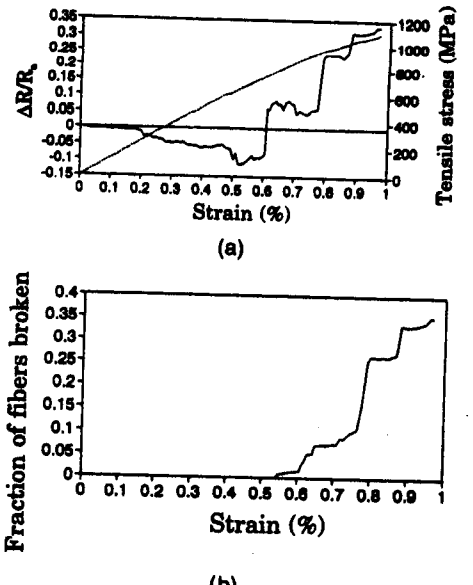

FIG. 14. Longitudinal stress, strain, and fractional resistance increase ($\Delta R/R_0$) obtained simultaneously during static tension up to fracture, which occurs at the highest strain in the curves, for continuous fiber epoxy-matrix composite. Solid curve: $\Delta R/R_0$ versus strain. Dashed curve: tensile stress versus strain. (b) Fraction of fibers broken versus strain during longitudinal tension up to fracture, obtained from $\Delta R/R_0$ curve in (a).

The effect of fiber damage on the electrical resistivity (Sec. II) was taken into account in obtaining Fig. 14(b). When 35% of the fibers were broken, the composite failed.

Figure 15 shows the longitudinal stress and strain and the through-thickness $\Delta R/R_0$ obtained simultaneously during cyclic longitudinal tension at a stress amplitude equal to 14% of the breaking stress. As expected, the strain returned to zero at the end of each cycle. The through-thickness $\Delta R/R_0$ increased upon loading and decreased upon unloading in every cycle, such that R irreversibly decreased slightly after the first cycle (i.e., $\Delta R/R_0$ did not return to 0 at the end of the first cycle). Upon increasing the stress amplitude, the effect was similar, except that the reversible part of $\Delta R/R_0$ was larger.

Figure 16 shows the longitudinal stress and strain and through-thickness $\Delta R/R_0$ obtained simultaneously during static longitudinal tensile loading up to fracture. The through-thickness $\Delta R/R_0$ increased abruptly with increasing strain for strains up to 0.8% and then increased gradually as the strain further increased up to failure, such that the through-thickness $\Delta R/R_0$ reached a maximum of 0.44.

The strain sensitivity (gage factor) is defined as the reversible part of $\Delta R/R_0$ divided by the longitudinal strain amplitude. It is negative (from −18 to −12) for the longitudinal $\Delta R/R_0$ and positive (17–24) for the through-thickness $\Delta R/R_0$. The magnitudes are comparable for the longitudinal and through-thickness strain sensitivities. As a result, whether the longitudinal R or the through-thickness R is preferred for strain sensing just depends on the convenience of electrical contact application for the geometry of the particular smart structure.

Cyclic compressive loading along the fiber direction was performed on the $[0]_{24}$ laminate. Figure 17 shows the compressive stress, strain, and longitudinal $\Delta R/R_0$ obtained simultaneously during cyclic compression at stress amplitudes equal to 14% of the breaking stress. The longitudinal $\Delta R/R_0$ increased upon compressive loading and decreased upon unloading in every cycle,

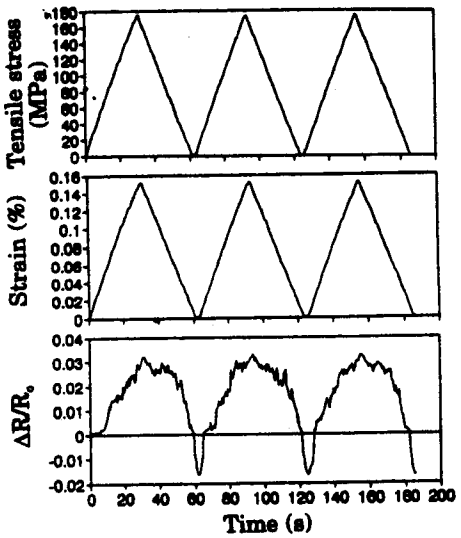

FIG. 15. Longitudinal stress and strain and the transverse $\Delta R/R_0$ obtained simultaneously during cyclic tension at a stress amplitude equal to 14% of the breaking stress for continuous fiber epoxy-matrix composite.

such that resistance R irreversibly increased very slightly after the first cycle. The magnitude of the gage factor was lower in compression (−1.2) than in tension (from −18 to −12).

Figure 18 shows longitudinal stress, strain, and $\Delta R/R_0$ obtained simultaneously during static longitudinal compressive loading. The electrical resistance was observed to increase monotonically with the compressive strain. After 0.7% compressive strain, the resistance increased abruptly. It is known that, when a unidirectional fiber composite is compressively loaded in the fiber direction, fibers will lose their stability first and get more wavy. When the compressive stress increases, the fibers will kink. With further increasing compressive loading, the fibers will fracture. At strains below 0.7% (Fig. 18), the resistance increase is probably partly due to the increased fiber stress upon compression and the consequent microstructural change and reversible increase in fiber resistivity. Beyond 0.7% strain, the rapid increase in electrical resistance is attributed to fiber fracture due to fiber kinking.

Figure 19 shows the through-thickness resistance versus compressive strain during longitudinal compression. The through-thickness resistance was observed to decrease at strains below 0.8%, and then increase with

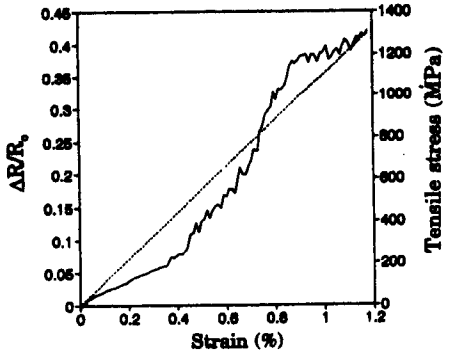

FIG. 16. Longitudinal stress and strain and the transverse $\Delta R/R_0$ obtained simultaneously during static tension up to fracture, which occurs at the highest strain in the curves, for continuous fiber epoxy-matrix composite. Solid curve: $\Delta R/R_0$ versus strain. Dashed curve: tensile stress versus strain.

further strain until the specimen failed. The decrease in through-thickness resistance is attributed to more fiber-fiber contacts due to the increased degree of waviness of the fibers. Beyond 0.8% strain, the increase in resistance is due to fiber fracture.

A dimensional change without any resistivity change would have caused longitudinal R to increase during tensile loading and decrease during compressive loading. In contrast, the longitudinal R was observed to decrease upon tensile loading and increase upon compressive loading. In particular, the observed magnitude of $\Delta R/R_0$ under tension was 7–11 times that of $\Delta R/R_0$ calculated by assuming that $\Delta R/R_0$ was due only to dimensional change and not due to any resistivity change. Hence, the contribution of $\Delta R/R_0$ from the dimensional change is negligible compared to that from the resistivity change.

For the longitudinal $\Delta R/R_0$ under tension, the gage factor is negative, in contrast to the positive values for a single carbon fiber (Sec. II) and for a short carbon fiber epoxy-matrix composite (Sec. IV). On the other hand, the gage factor is negative for a single carbon fiber in epoxy (Sec. III). In a polymer-matrix composite, the thickness of the polymer between adjacent fibers is much less than that of the polymer embedding a single fiber, so the residual stress in the fibers of the composite is much less than that of a single fiber in the polymer. Therefore, the origin of the electromechanical effect observed for the polymer-matrix composite with continuous carbon fibers is not the same as those of the electromechanical effects of Secs. II–V.

The decrease in longitudinal $\Delta R/R_0$ and increase in through-thickness $\Delta R/R_0$ upon longitudinal tension and the increase in longitudinal $\Delta R/R_0$ and decrease

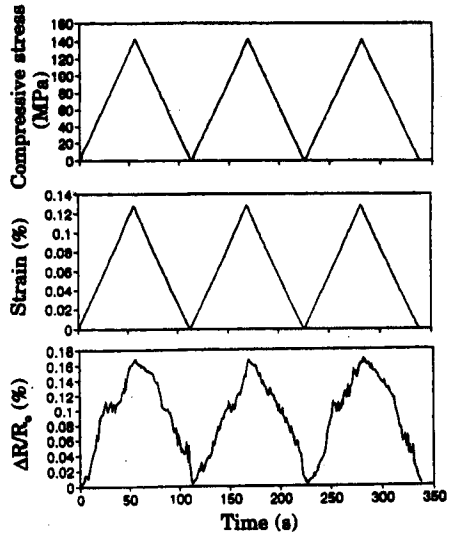

FIG. 17. Longitudinal stress, strain, and $\Delta R/R_0$ obtained simultaneously during cyclic compression (longitudinal) at a stress amplitude equal to 14% of the breaking stress for continuous fiber epoxy-matrix composite.

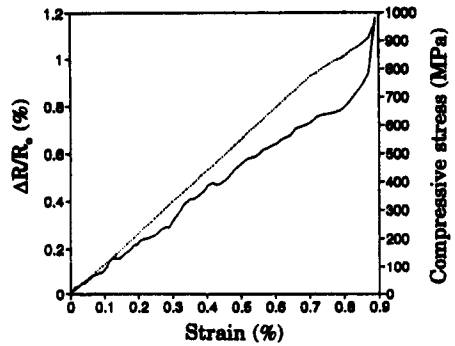

FIG. 18. Longitudinal stress, strain, and $\Delta R/R_0$ obtained simultaneously during static compression (longitudinal) up to fracture, which occurs at the highest strain in the curves, for continuous fiber epoxy-matrix composite. Solid curve: $\Delta R/R_0$ versus strain. Dashed curve: compressive stress versus compressive strain.

in transverse $\Delta R/R_0$ upon longitudinal compression is observed in this section for a continuous carbon fiber composite in cyclic loading (Figs. 13, 15, and 17) or static loading at low strains (Figs. 14, 16, 18, and 19)

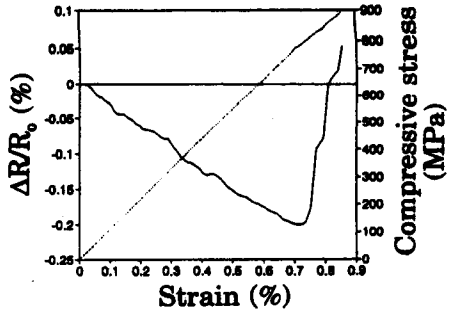

FIG. 19. Longitudinal stress and strain and transverse $\Delta R/R_0$ obtained simultaneously during static compression (longitudinal) up to fracture, which occurs at the highest strain in the curves, for continuous fiber epoxy-matrix composite. Solid curve: $\Delta R/R_0$ versus strain. Dashed curve: compressive stress versus compressive strain.

and tentatively attributed to (i) the increase in the degree of alignment (decrease in the degree of waviness) of the fibers upon longitudinal tension and the decrease in the degree of fiber alignment upon longitudinal compression, and (ii) the decrease in the compressive residual stress in the fibers upon longitudinal tension and increase in this stress upon longitudinal compression. The increase in the degree of alignment causes the longitudinal resistivity to decrease. In addition, it causes the adjacent fiber layers to have less chance of touching one another, so the transverse resistivity increases. The effects are almost totally reversible, when the strain is reversible. That the reversible part of $\Delta R/R_0$ is due to the increase in the degree of alignment of the fibers upon longitudinal tension is supported by the fact that the longitudinal tensile modulus decreases with increasing magnitude of the reversible part of $\Delta R/R_0$[22] and that the longitudinal tensile modulus is known to decrease with decreasing degree of alignment of the fibers. In other words, the lower the degree of alignment of the fibers under no load, the greater the magnitude of the reversible part of $\Delta R/R_0$. Also consistent with the notion that the reversible part of $\Delta R/R_0$ is due to the increase in the degree of alignment of the fibers upon longitudinal tension is the observation that the absolute value of the reversible part of the longitudinal $\Delta R/R_0$ increases with increasing longitudinal resistivity at no load, and that the reversible part of through-thickness $\Delta R/R_0$ decreases with increasing through-thickness resistivity at no load, since the longitudinal resistivity is expected to decrease with increasing degree of fiber alignment while the through-thickness resistivity is expected to increase with increasing degree of fiber alignment.[22]

The irreversible behavior, though small compared to the reversible behavior, is such that R (longitudinal

or through-thickness) under tension is irreversibly decreased after the first cycle. This behavior is attributed to the irreversible disturbance to the fiber arrangement at the end of the first cycle, such that the fiber arrangement becomes less neat. A less neat fiber arrangement means more chance for the adjacent fiber layers to touch one another.

The stepwise increase of the longitudinal $\Delta R/R_0$ in the large strain regime (Fig. 14) is attributed to fiber breakage, which probably occurs in spurts. Such a stepwise increase had been previously observed and is also attributed to fiber breakage.[23]

The through-thickness $\Delta R/R_0$ increases abruptly at intermediate strains but increases gradually at high strains (Fig. 16). This is because only a small change in the degree of fiber alignment causes a large change in the chance of adjacent fiber layers to touch one another. Moreover, fiber breakage, which occurs at high strains, essentially does not affect transverse $\Delta R/R_0$ (Fig. 16), but affects longitudinal $\Delta R/R_0$ (Fig. 14).

VII. CONCLUSION

Because of its electrical conductivity, carbon fiber provides strain sensing through the change in electrical resistance/resistivity upon strain. However, the nature and origin of the electromechanical effect depend on the matrix around the fiber and the continuity of the fiber. A single bare carbon fiber is a resistive strain sensor with a gage factor of 1.9–2.3. The effect is merely due to a change in dimensions of the fiber upon tension; it is not due to a change in resistivity. A single carbon fiber embedded in epoxy is a piezoresistive strain sensor with a gage factor of −17. The effect is due to a reduction in the residual compressive stress in the fiber upon tension; the residual stress is caused by the shrinkage of the epoxy during curing and subsequent cooling. A single carbon fiber embedded in cement does not experience this residual stress. An epoxy-matrix composite containing randomly oriented short carbon fibers (5.5 vol%) is a piezoresistive strain sensor with a gage factor of 6–23 under tension and 29–31 under compression; the effect is due to the change in proximity between adjacent fibers upon strain. A cement-matrix composite containing randomly oriented short carbon fibers (0.2–0.5 vol%) is a piezoresistive strain sensor with a gage factor of at least 500 under compression or tension; the effect is due to slight fiber pullout upon tension and slight fiber push-in upon compression. An epoxy-matrix composite containing continuous unidirectional carbon fibers (58 vol%) is a piezoresistive strain sensor with a gage factor from −12 to −18 in the longitudinal direction and from 17 to 24 in the through-thickness direction under longitudinal tension, and from 1.1 to 1.3 in the longitudinal direction under longitudinal compression; effects in both directions are tentatively due to an increase in the degree of fiber alignment and decrease in fiber residual stress upon longitudinal tension.

ACKNOWLEDGMENTS

This work was supported in part by the National Science Foundation and Sensor Plus Inc. (Amherst, NY). Technical assistance by Mr. Xiaohui Li of State University of New York at Buffalo is acknowledged.

REFERENCES

1. P.C. Conor and C.N. Owston, Nature (London) **223**, 1146 (1969).
2. C.N. Owston, J. Phys. D **3**, 1615 (1970).
3. C.A. Berg, H. Cumpston, and A. Rinsky, Textile Res. J. **42** (8), 486 (1972).
4. S.J. DeTeresa, Carbon **29** (3), 397 (1991).
5. A.S. Crasto and R.Y. Kim, Proc. Am. Soc. Composites, 8th Tech. Conf. (Technomic Pub Co., Lancaster, PA, 1994), pp. 162–173.
6. N. Muto, H. Yanagida, M. Miyayama, T. Nakatsuji, M. Sugita, and Y. Ohtsuka, J. Ceram. Soc. Jpn. (Int. Ed.) **100**, 582 (1992).
7. J. Kost, M. Narkis, and A. Foux, J. Appl. Polym. Sci. **29**, 3937 (1984).
8. S. Radhakrishnan, S. Chakne, and P.N. Shelke, Mater. Lett. **18**, 358 (1994).
9. P.K. Pramanik, D. Khastgir, S.K. De, and T.N. Saha, J. Mater. Sci. **25**, 3848 (1990).
10. X. Wang and D.D.L. Chung, Smart Mater. Struct. **4**, 363 (1995).
11. P. Chen and D.D.L. Chung, Composites Part B **27B**, 11 (1996).
12. P. Chen and D.D.L. Chung, Smart Mater. Struct. **2**, 22 (1993).
13. P. Chen and D.D.L. Chung, J. Am. Ceram. Soc. **78** (3), 816 (1995).
14. P. Chen and D.D.L. Chung, ACI Mater. J. **93** (4), 341 (1996).
15. P. Chen and D.D.L. Chung, J. Electron. Mater. **24** (1), 47 (1995).
16. P. Chen, X. Fu, and D.D.L. Chung, ACI Mater. J. **94** (2), 147 (1997).
17. X. Fu and D.D.L. Chung, Cem. Concr. Res. **26** (1), 15 (1996).
18. X. Fu and D.D.L. Chung, Cem. Concr. Res. **27** (9), 1313 (1997).
19. P. Chen and D.D.L. Chung, ACI Mater. J. **93** (2), 129 (1996).
20. X. Fu and D.D.L. Chung, Cem. Concr. Res. **25** (7), 1391 (1995).
21. X. Fu, W. Lu, and D.D.L. Chung, Cem. Concr. Res. **28** (2), 183 (1998).
22. X. Wang and D.D.L. Chung, Smart Mater. Struct. **5**, 796 (1996).
23. K. Schulte and Ch. Baron, Composites Sci. Technol. **36**, 63 (1989).